Journal of Physics: Conference Series **717** (2016) 012077 doi:10.1088/1742-6596/717/1/012077

Efficient fast electron generation in an interaction of Intense, ultrashort laser with metal nanoparticle coated dielectric target

Deep Sarkar, Sheroy Tata, Moniruzzaman Shaikh, Amit D. Lad, Amitava Adak, Subhrangsu Sarkar , Pushan Ayyub and G. Ravindra Kumar

Tata Institute of Fundamental Research, Mumbai, India.

Email: deep.sarkar@tifr.res.in

Abstract. Hot electron generation in intense laser-matter interaction studies is a topic of great interest due in significant part to its applications in fast ignitor scheme in Inertial Confinement Fusion (ICF). We measure the hot electron energy spectrum from Ag nanoparticle coated fused silica target (100 µm thick) interacting with an intense (I~$10^{18}\mathrm{W/cm^2}$), short pulse (τ~ 30×10^{-15}s) laser and compare the results with those of an uncoated fused silica. Enhancement in hot electron energy and hard x-ray yield is measured as a function of thickness of Ag nano-coating, varied from tens of nm to hundreds of nm. The hot electron temperatures and integrated x-ray yield are observed to be greater for subwavelength film thicknesses for the case of a p-polarized laser. Such results indicate that metal nanoparticle layers have an important role to play in the enhancement of laser-plasma coupling efficiency for short scale-length plasmas created in femtosecond laser interactions.

1. Introduction

An intense, ultrashort, laser pulse interacting with solid matter creates a solid density plasma via different ionization mechanisms [1] and couples with the plasma thereafter via collective processes engendering the generation of hot electron jets [2], ion acceleration [3], ultrashort X-ray pulses [4], high harmonics [5] and other kinds of radiation such as Cherenkov [6] and THz radiation [7]. Several standard diagnostics are employed to determine the efficiency of coupling between the laser light and the pre-ionized hot, dense matter. One such diagnostic is Electron Spectrometry (ESM) [8] which characterizes the energy spectra of the hot electrons. The distribution curve is a typical bi-Maxwellian [9] exhibiting two temperatures. The hot electron temperature T_{hot} may scale either as the square root [10] or one-third power [11] of the laser intensity depending on the dominant absorption mechanism.

Measurement of integrated X-ray yield (bremsstrahlung and $K_{\propto}$ emission) is another diagnostic of the laser-plasma coupling efficiency as higher yield in X-rays imply greater absorption which in turn implies hotter electrons. Structured targets [12] such as nanorod arrays [13], nanometric subwavelength gratings [14] and microstructures [15] are known to enhance the conversion efficiency of laser energy into x-rays and hot electrons. Such an enhancement is attributed to the local electric field enhancement of several orders of magnitude at the surface structures due to the “lightning rod effect” [16]. Consequently, multifold enhancement in X-ray yield has been observed for such structured samples [12-15].

In our experiment, we have investigated the effect of sputter deposited layers of Ag nanoparticles with subwavelength thickness (~ 30-100 nm) on the laser energy conversion efficiency by measuring the hot electron spectrum by ESM and X-ray yield as a function of film thickness. The hot electron temperatures and x-ray yields for different film thicknesses have been compared with that of a plane, uncoated fused silica target of thickness $100\mu m$ which also serves as a substrate for the coated targets.

In the next section, we describe our experimental set-up in detail following which we present our findings and discuss their implications. A summary is presented in subsection 2.1.

2. Experimental setup

The experiment was performed with the 100 TW laser facility at TIFR (Ti: Sapphire, 800nm central wavelength) which delivers 25 fs pulses at a repetition rate of 10 Hz. The ASE contrast of the pulse was measured to be ~10^{10}. The laser beam is focused onto the target to a spot size of 10 μm (FWHM) using an (f/2.5) Off-axis parabolic mirror. ESMs were placed along target front, target rear and laser direction simultaneously to obtain information on the dominant heating mechanism. A NaI (Tl doped) detector coupled with a photomultiplier tube was placed at the target front at a distance of 90cm from the target surface. To reduce counts due to noise from cosmic particles, the detector was placed inside a thick lead cylinder and lead apertures were used to avoid saturation and pile-up due to excess X-ray flux. A schematic of the experimental setup is shown below (Fig.1).

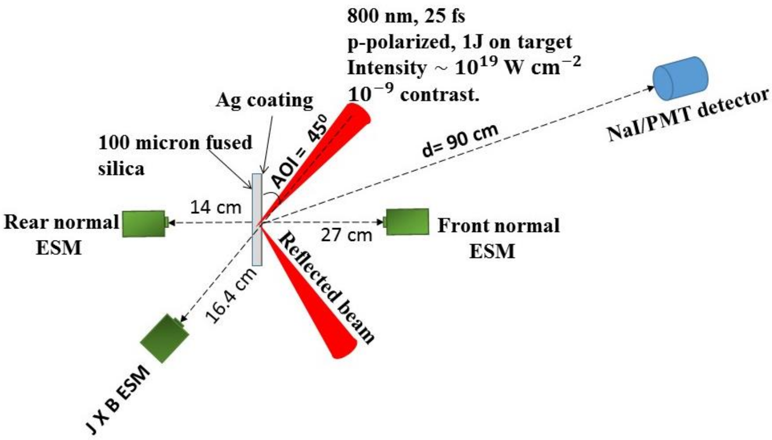

Fig. 1. **Schematic of experimental setup**.

As shown in Fig. 1, the laser beam was incident on the target sample at 45° angle of incidence, with its electric field polarized in the plane of incidence (p-polarized). The intensity on target was ~$10^{18}\mathrm{W/cm^2}$. Both the electron energy spectra and the integrated X-ray yield were averaged over a total of around 30-40 shots for the coated samples and 70 shots for the plane FS sample.

Journal of Physics: Conference Series **717** (2016) 012077 doi:10.1088/1742-6596/717/1/012077

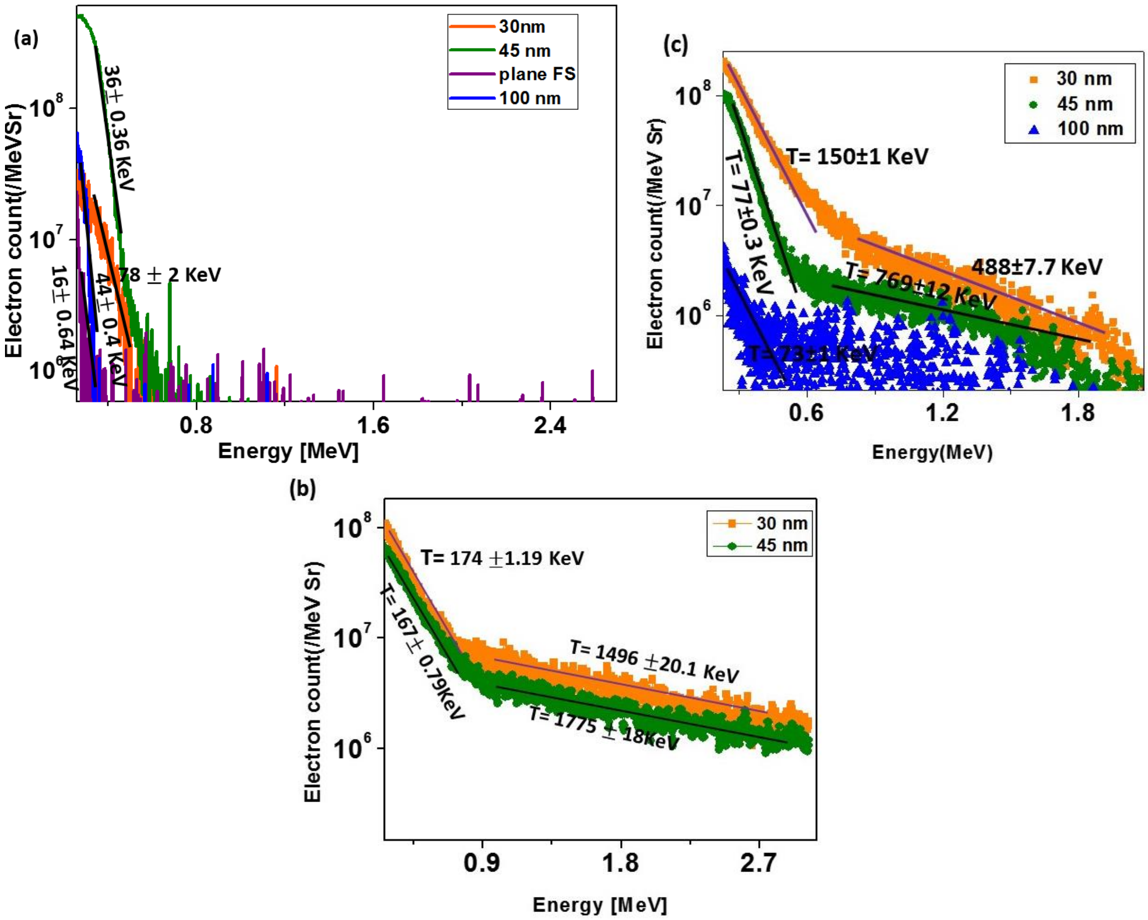

Fig. 2. (a) Energy spectrum along target front normal (b) Hot electron energy spectrum for 30 nm (orange) and 45 nm (green) coating thickness along J×B direction. (c) ESM energy spectrum along target rear normal (no trace obtained for plane FS).

Results. Fig. 2 shows the electron energy spectra for the coated and plane targets along the three directions. Along all three directions, target with film thicknesses around 30–45 nm yield electrons with highest temperatures. The temperatures are highest along the J×B direction, revealing J×B heating as the dominant heating mechanism for our case. The above trend clearly indicates a role of film thickness in optimizing the laser energy coupling efficiency with the plasma. The significantly lower electron temperatures in case of 100 nm film coated target, on the other hand, seems to imply the thickness dependence is weak or altogether absent for coating thicknesses above 100nm.

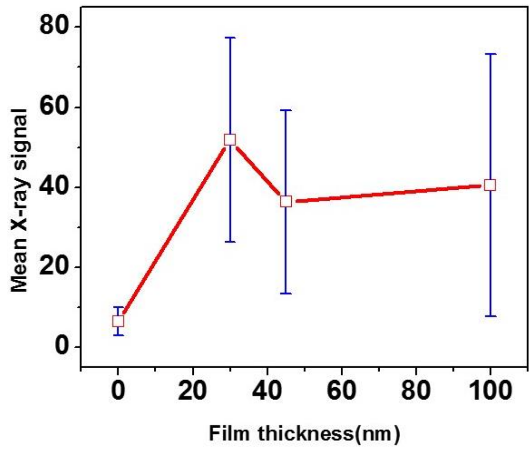

Fig. 3. Integrated x-ray yield as a function of coating thickness

The X-ray yield result (Fig.3) show a similar trend of enhancement for the nanocoated targets but the thickness dependence is not prominent due to large error bars in the yield values owing to statistical fluctuations in the X-ray signal. This may be due to the X-rays being generated both from the coating and the substrate interface.

2.1. Discussion

In our experiment, we have assumed absence of any laser instability mechanism (TPD, SRS) affecting the x-ray and hot electron generation, due to the extremely high contrast (~ 10^{10} ns contrast) of the laser pulse [17] and requirement of high threshold intensity for the SRS [18] to occur. Further, all ion motions and related instabilities (ion-acoustic waves, Langmuir decay instability) were ignored due to the extremely short time-scales of interaction involved.

In summary, we performed an experimental investigation of laser-plasma coupling efficiency in Ag nanoparticulate coatings for intense, femtosecond pulses by measuring the hot electron energy spectrum and time integrated X-ray yield and compared the results with that of a bare FS target. It was found that the electron temperatures were the highest for 30 and 45 nm film thickness with J×B heating as the dominant acceleration mechanism. The X-ray yield was higher for coated targets as compared to the plane one by about 5 orders of magnitude but the thickness dependence of the enhancement was unclear due to large statistical fluctuations in the signal. These results indicate the presence of a length scale besides the morphology of the coating which must be taken into account to control the generation of hot electrons in a high intensity laser-matter interaction. However, for an accurate physical interpretation of the underlying mechanism, simulations are required.

References

[1] P. Gibbon, *Short Pulse Laser Interactions with Matter An Introduction* (Imperial College Press, 2005) ; M. Protopapas *et al.,* Rep. Prog. Phys. **60** (1997).
[2] L. Gremillet *et al.*, Phys. Rev. Lett. **83,** 5015 (1999).
[3] M. Hegelich *et al.,* Phys. Rev. Lett. **89,** 085002 (2002).
[4] J.D. Kmetec *et al.,* Phys. Rev. Lett. **68,** 1527 (1992).
[5] A. Tarasevitch *et al.,* Phys. Rev. A **62,** 023816 (2000); M. Zepf *et al.,* **58,** R5253 (1998).
[6] F. Brandl *et al.,* Europhys. Lett., **61** (5), 232 (2003).
[7] H. Hamster *et al.,* Phys. Rev. Lett. **71,** 2725 (1993).
[8] K.A. Tanaka *et al.,* Rev. Sci. Instrum. **76,** 013507 (2005).
[9] Estabrook & Kruer, Phys. Rev. Lett. **40,** 42(1978).
[10] S.C. Wilks *et al.,* Phys. Rev. Lett., **69,** 1383 (1992).
[11] F. Beg *et al.,* Phys. Plasmas **4,** 447 (1997).
[12] P.P. Rajeev *et al.,* Phys. Rev. Lett. **90,** 115002 (2003).
[13] S. Mondal *et al.,* Phys. Rev. B **83,** 035408 (2011).
[14] S. Kahaly *et al.,* Phys. Rev. Lett. **101,** 145001 (2008).
[15] M. Krishnamurthy *et al.,* Optics Express **20,** 5754 (2012).
[16] P.P. Rajeev *et al.,* Opt. Lett. **29,** 2662-2664 (2004).
[17] F. Baffigi *et al.,* Phys. Plasmas **21,** 072108 (2014).
[18] H.A. Baldis *et al.,* Phys. Fluids **26,** 1364 (1983).